Adaptive Buck-Boost Converter for RF Energy Harvesting and Transfer in Biomedical Applications

Gustavo C. Martins and Wouter A. Serdijn
Section Bioelectronics, Microelectronics Department, Delft University of Technology, Delft, The Netherlands
Email: g.martins@ieee.org, serdijn@ieee.org

***Abstract*—The continuous improvement in reducing the power consumption of electronic devices, including biomedical ones, makes the use of energy harvesting systems instead of batteries attractive. Conventionally, energy harvesting systems are optimized to operate in a single worst-case scenario. However, it is often the case that the available input power varies in different situations, which creates a need for energy converters that operates efficiently over a broader input power range. In this paper, a versatile buck-boost converter suitable for wireless energy harvesting and transfer is proposed. The converter maximizes the system's efficiency by maintaining its input resistance fixed during harvesting. Harvested energy is stored in a storage capacitor. The converter can be dynamically adjusted for different available input power and voltage levels. This is accomplished by employing pulse frequency modulation and reconfigurable power switches. A novel adaptively biased zero-current-detection comparator is employed to increase the converter's efficiency, its input having an offset that depends on the output voltage. The converter was simulated for input power levels from $1\,\mu\mathrm{W}$ to $1\,\mathrm{mW}$ and input voltage level from 0.38 to $1.3\,\mathrm{V}$. Its peak efficiency is 76.3% at an input power of $1\,\mu\mathrm{W}$ and 86.3% at $1\,\mathrm{mW}$.**

I. Introduction

The active circuitry of biomedical devices is often powered from batteries, which have a limited life time and/or must be charged from time to time. However, with the decreasing power consumption of the biomedical devices, energy harvesting techniques or wireless power transfer can be used as an alternative to batteries [1].

There are several modalities of energy harvesting, which include thermoelectric, solar and radio-frequency energy harvesting [2]. The harvester element captures energy from a source and generates an output voltage that depends on the available power. This voltage must be boosted and regulated in order to provide a stable supply for the electronics. The input resistance of this voltage booster should be set to optimize the harvester efficiency [3]. This optimum value is tracked using Maximum Power Point Tracking (MPPT) techniques. The voltage boosting converter must be designed to allow for changes in the input resistance while keeping a good conversion efficiency.

In this paper, we specifically tackle the problem of wireless energy harvesting and transfer. In Fig. 1, we present the block diagram of an energy converter that adapts itself to its varying input power. Two DC-DC converter blocks make the interface between the rectifier and the load. The first DC-DC converter extracts energy from the rectifier output and charges a storage capacitor. When enough energy is stored, it can be processed by the second DC-DC converter and relayed onto the load, which represents the target circuitry to be powered. If the available power is sufficiently high to continuously power the load, i.e., if no duty cycling is necessary, the DC-DC converter that charges the capacitor can be bypassed and the power is directly transferred from the rectifier to the load through the second DC-DC converter. Prior to the beginning of the harvesting operation, a start-up circuit starts the DC-DC converters and MPPT block.

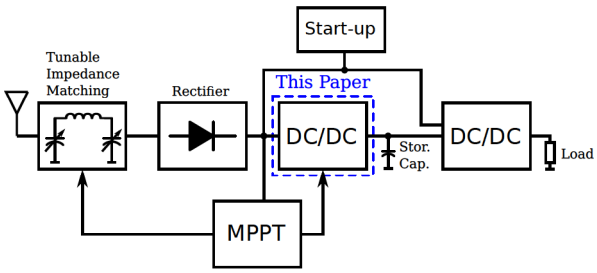

Fig. 1. Adaptive power conversion chain simplified block diagram.

In order to boost the voltage, a switched inductor DC-DC converter or a switched capacitor DC-DC converter can be used. While charging a storage capacitor, the output voltage will be increasing from the ground voltage up to the maximum possible. In the case of a switched capacitor converter, the maximum efficiency is obtained for specific values of the output voltage only, which depends on the selected converter configuration. In contrast, the switched inductor topologies can fundamentally operate with high efficiency for any output voltage. Moreover, if for the implementation of the switched inductor circuit a buck-boost converter is selected, its input resistance can be fixed in open-loop configuration, as will be further explained in Sec. II.

Several low-power biomedical devices have an average power consumption below $1\,\mathrm{mW}$ [4], [5], [6], which makes the use of wireless energy transfer and harvesting suitable. In this work, we propose a buck-boost converter for use in such power conversion chains that can operate efficiently for available input power levels from $1\,\mu\mathrm{W}$ to $1\,\mathrm{mW}$. A description of the circuits employed in the converter is presented in Sec. II. In Sec. III, we present the simulation results of the buck-boost converter and comparison with previous works. Finally, the conclusion of this work is presented in Sec. IV.

II. Buck-Boost Converter Description

In order to keep the input resistance of the DC-DC converter fixed while charging a capacitor, the input current must be independent of the output voltage. This can be performed

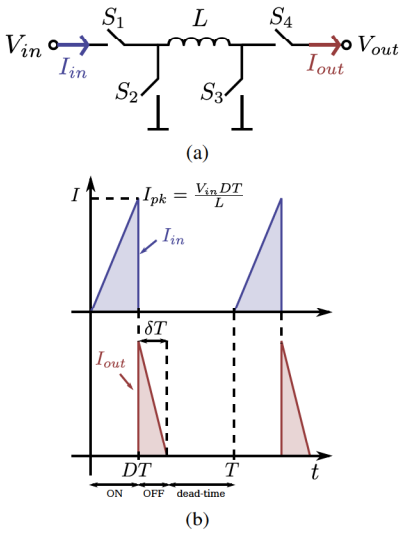

Fig. 2. (a) Buck-boost converter circuit principle; (b) Input and output current in DCM.

using a buck-boost converter operating in Discontinuous Conduction Mode (DCM) and open loop, such as the non-inverting buck-boost converter in Fig. 2(a). It has an input current I_{in} (see Fig. 2(b)) that is independent of the output voltage V_{out}. This behaviour cannot be achieved with the straight-forward boost converter. The average input resistance of the buck-boost converter in DCM, neglecting the input voltage ripple, is given by:

$$R_{in,avg} = \frac{V_{in}}{I_{in,avg}} = \frac{2L}{D^2T}, \tag{1}$$

in which D is the duty cycle of the switching control signal (DT is the ON-time of the converter), L is the inductor value and T is the switching period.

Even though the same converter can be used in other energy harvesting systems, we optimized its design for a wireless energy harvesting system that employs a single-stage differential-drive CMOS rectifier [7]. The optimum output voltage of the employed rectifier varies from 0.38 V at 1-μW output power to 1.3 V at 1-mW output power. The technology used in this design is a standard 0.18-μm technology, with a maximum V_{DD} of 1.8 V. Those are the basic specifications in which the buck-boost converter must operate.

The proposed converter's block diagram is presented in Fig. 3. Since V_{out} increases with the charging of the storage capacitor, the inductor discharge time δT also changes every cycle ($\delta T = LI_{pk}/V_{out}$). With that in mind, we decided to employ an asynchronous zero current detection scheme. A level shifter is used to shift the voltage V_d at one of the inductor's node (see Fig. 3) and the ground voltage to a suitable level for the adatively biased comparator, thereby detecting when the current through the inductor is zero. In order to be able to convert all the power in the available input power range, a pulse frequency modulation scheme is employed. An oscillator has its frequency digitally controlled through a 9-bit input and its output is used to drive an ON-time generator, which generates a fixed ON-time. This signal is fed to the configurable power switches and to a control block that initiates the OFF-time and, via the output of the zero current

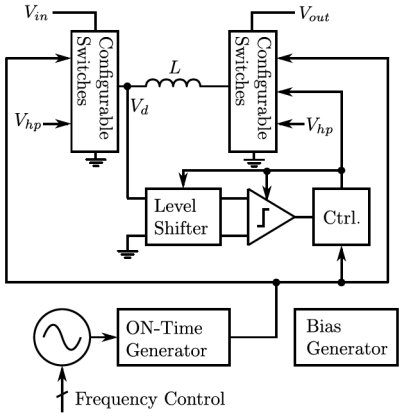

Fig. 3. Block diagram of the proposed converter.

detector, makes the decision on when to initiate the dead-time of the power switches. The signal V_{hp} is derived from the 9-bit oscillator control signal and sets the power switches into either high- or low-power configuration. The employed power inductor L is a 220-μH inductor with a parasitic series DC resistance of 21.1 Ω (Coilcraft XPL2010-224ML).

A. Adaptively Biased Comparator

An adaptively biased amplifier is presented in [8], in which the bias current increases with the differential input V_{in} in order to increase slew rate. We use a similar approach, but apply it to a comparator to increase the bias current when V_{in} approaches zero, in order to decrease the time the comparator takes to bring the output from ground to V_{dd}. The proposed circuit is presented in Fig. 4. Resistor R_1 has been added in order to create a non-linearity in the feedback loop and be able to increase the multiplying factor of the current mirror M_5-M_6 and while ensuring stability of the circuit during the OFF-time phase.

Input V_i^+ is connected to the shifted value of V_d (in Fig. 3), which increases as the inductor current decreases, while input V_i^- is connected to the shifted value of the ground voltage, which is fixed. As V_i^+ increases, and gets closer to V_i^-, the current through M_1 increases and so does the tail current I_T through the positive feedback. Furthermore, the differential pair M_3-M_4 makes the I_T versus V_{in} curve steeper by multiplying the current in the feedback path by an extra term dependent on V_{in}. This decreases the average power consumption. This comparator has a delay of 9.1 ns and an average power consumption of 10.1 nW for the converter operating at $P_{in} = 1\,\mu$W and $V_{out} = 1.8$ V, according to circuit simulations, which is small enough to not have a large influence on the converter efficiency.

B. Level Shifter and Offset Generator

Even though the speed of the comparator is high, there are still sources of delay that cannot be mitigated, such as the switching delay of the power switches or the phase delay between the inductor current I_L and the V_d voltage. If a small offset is added to the comparator input, it can compensate for these delays by switching off the inductor at a time T_d before the current falls to zero and, thus, increase the conversion

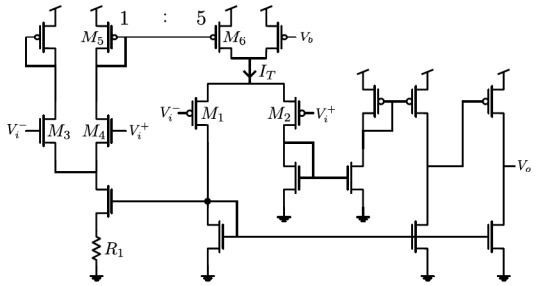

Fig. 4. Circuit schematic of the adaptively biased comparator used for zero current detection.

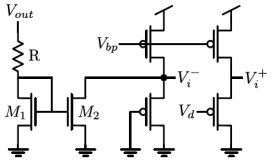

Fig. 5. Circuit schematic of the level shifter with offset generation.

efficiency. The time T_d depends neither on the converter output voltage V_{out} nor on the inductor peak current. Since the inductor discharge time is dependent on V_{out} (and so is the rate of change of V_d), the offset must also change with V_{out} in order to compensate for the fixed T_d:

$$V_{off} = V_{out}\frac{T_d R_{on}}{L}, \tag{2}$$

in which R_{on} is the ON resistance of the switch that connects V_d to ground while the inductor current is decreasing.

To generate an offset that is dependent on the output voltage and to shift the input voltages to a level that is suitable to the comparator, the circuit in Fig. 5 is proposed. The current mirror formed by M_1-M_2 subtracts a current that depends on V_{out} from the level shifter branch that has its input connected to ground. This makes the output voltage of this branch decrease as V_{out} increases. The resistor R is an off-chip 47-MΩ resistor.

C. Configurable Switches

The power switches S_1 to S_4 (in Fig. 2(a)) are implemented by switches connected in parallel (not shown here). Wider switches are used for operation when $P_{in} > 500\,\mu$W and smaller switches otherwise. When the input power is low, only the smaller switches are used in order to reduce the power needed to drive them. Alternatively, we could reduce the switching losses exclusively by decreasing the switching frequency. This, however, would increase the peak value of I_L, which, in turn, would lead to increased conduction losses. Unless a larger inductor is used, which is undesired.

D. Frequency Modulation and ON-Time Generator

The oscillator topology is presented in Fig. 6(a). The 9-bit input $V_{s0..8}$ controls the current employed to charge and discharge the capacitor through a current starved inverter, modulating its frequency. A Schmitt trigger, presented in Fig. 6(b), is used to control whether the capacitor is being charged or discharged, thus generating an oscillation. To decrease the

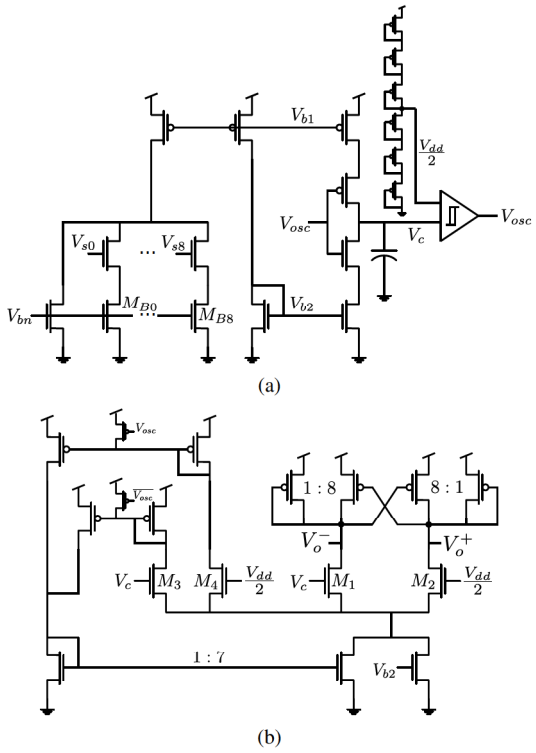

Fig. 6. Schematics of the oscillator (a) and the first stage of the Schmitt trigger (b).

average power consumption of this block, we also use the adaptive biasing technique. Transistors M_3-M_4 generate a scaled copy of the currents flowing through M_1-M_2, and are 4 times smaller. The signal V_{osc} is the Schmitt trigger output and it controls which branch of the feedback loop is operating, switching the direction in which the bias current increases. The oscillator must be set to an optimum frequency by the MPPT circuit. The oscillator frequency can be modulated with a 2.5 kHz step through the binary-weighted current mirrors (M_{B0}-M_{B8}), and its minimum and maximum frequencies are approximately 10 kHz and 1.3 MHz, respectively. This frequency must be set to 20 kHz for $P_{in} = 1\,\mu$W and to 1 MHz for $P_{in} = 1$ mW. The power consumption of this oscillator is 36 nW at 20 kHz. Bias voltage V_{b2} is used to bias the Schmitt trigger as well as making it faster as the oscillator frequency increases. Doing so, the comparator's power consumption also increases, but it does not affect the efficiency since the available input power is expected to be higher when higher frequencies are employed.

A fixed, 440-ns ON-time is generated by charging a capacitor and comparing its voltage to a reference. The ON-time starts at the rising edge of the oscillator output. The power consumption of this circuit is 26 nW when operating at 20 kHz.

E. Bias Generator

In order to bias all the blocks, an all-MOS current reference generator [12] is employed. Additional current mirrors are used to multiply the current and bias the more power hungry circuits, which perform the zero current detection. This circuit consumes 9 nW from a power supply voltage of 1.8 V.

TABLE I. PERFORMANCE SUMMARY OF THE BUCK-BOOST CONVERTER AND COMPARISON

Parameter	[9]	[10]	[11]	This work
Technology	0.18 μm	0.18 μm	Discrete	0.18 μm
Peak efficiency (at P_{in})	66.8% (16.9 μW)	83.4% (299.7 μW)	76% (19 μW)	76.3% (1 μW) / 86.3% (1 mW)
Input voltage	0.3-0.7 V	0.1 V	0.38-1.5 V	0.38-1.3 V
Power range	15-125 μW (input)	25 μW-1 mW (output)	$\sim$ 4-70 μW (input)	1 μW-1 mW (input)
Max. output voltage	2 V	0.5 V	2 V	1.8 V
Quiescent power	3.12 μW	480 nW	7.8 μW	133 nW
Inductor size	1 mH	1 mH	10 mH	220 μH
Converter topology	Boost converter	Boost converter	Buck-boost converter	Buck-boost converter

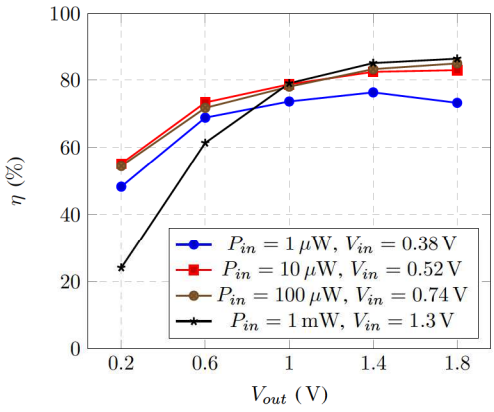

Fig. 7. Efficiency results of the buck-boost converter for various output voltages.

III. RESULTS

This section presents the results of circuit simulations of the converter system discussed previously. Since the main application of this buck-boost converter is to charge a storage capacitor in an energy harvesting system while maintaining good efficiency for different available power levels, we present the efficiency results for a varying output voltage from 0.2 to 1.8 V in Fig. 7 (V_{in} is the optimum voltage for the rectifier, as explained in Sec. II). The peak efficiency of the buck-boost converter is 76.3% at an input power of 1 μW and 86.3% at 1 mW. While charging a capacitor from 0.2 to 1.8 V, the total efficiency is 73.8% at $P_{in} = 1\,\mu$W. The lower efficiency at lower output voltages is observed because the OFF-time is larger (voltage drop across the inductor is lower) and the zero current detection circuitry is turned on for a longer time. Additionally, the output power switches are not optimized for low output voltages. This extra conduction loss is more prominent at higher P_{in}, because I_L is larger.

In Tab. I, we present the performance summary of the buck-boost converter and a comparison with other DC-DC converters applied in energy harvesting systems. The system designed in this work presents a high efficiency for a larger range of available input power, it has lower quiescent power consumption and it employs the smallest inductor of all works.

IV. CONCLUSION

We have presented a buck-boost converter optimized for a wireless energy transfer and harvesting system, but that could also be applied in other energy harvesting modalities, in which the converter is used to charge a storage capacitor. The converter presents an optimum load for the rectifier for all output voltage levels, optimizing its efficiency during the capacitor charging. The converter operates from $P_{in} = 1\,\mu$W to 1 mW, which makes it suitable for several biomedical applications. The converter presents competitive performance when compared to the state-of-the-art converters and is a good solution for optimizing the power conversion chain of wireless energy harvesting systems. All results presented in this paper are outcome of schematic simulations and the overall system efficiency also depends on other blocks that were not discussed, but this work shows a direction in order to obtain higher-efficiency wireless energy transfer systems that operate over a broader available input power range.

ACKNOWLEDGMENTS

This work was supported by CAPES Foundation, Brazil. We would like to thank Dr. Vasiliki Giagka and Alessandro Urso for their valuable discussions and contributions.

REFERENCES

[1] Y. Manoli, "Energy harvesting - from devices to systems," in *Proc. IEEE Eur. Solid State Circuits Conf. (ESSCIRC)*, Sept. 2010, pp. 27–36.

[2] R. Vullers, R. Schaijk, H. Visser, J. Penders, and C. van Hoof, "Energy harvesting for autonomous wireless sensor networks," *IEEE Solid-State Circuits Magazine*, vol. 2, no. 2, pp. 29–38, 2010.

[3] T. Paing, J. Shin, R. Zane, and Z. Popovic, "Resistor emulation approach to low-power RF energy harvesting," *IEEE Trans. Power Electronics*, vol. 23, no. 3, pp. 1494–1501, 2008.

[4] A. Mansano, Y. Li, S. Bagga, and W. Serdijn, "An autonomous wireless sensor node with asynchronous ECG monitoring in 0.18μm CMOS," *IEEE Trans. Biomed. Circuits Syst.*, vol. 10, no. 3, pp. 602–611, 2016.

[5] E. Greenwald, E. So, M. Mollazadeh, C. Maier, R. Etienne-Cummings, N. Thakor, and G. Cauwenberghs, "A 5μW/channel 9b-ENOB BioADC array for electrocortical recording," in *2015 IEEE Biomedical Circuits and Systems Conf. (BioCAS)*, Oct. 2015.

[6] M. M. Ghanbari, J. M. Tsai, and S. Gambini, "An energy-efficient heterogeneously-integrated capacitive pressure sensing system," in *2015 IEEE Biomedical Circuits and Systems Conf. (BioCAS)*, Oct. 2015.

[7] K. Kotani, A. Sasaki, and T. Ito, "High-efficiency differential-drive cmos rectifier," *IEEE J. Solid-State Circuits*, vol. 44, no. 11, pp. 3011–3018, 2009.

[8] M. G. Degrauwe, E. A. Vittoz, and H. J. de Man, "Adaptive biasing CMOS amplifiers," *IEEE J. Solid-State Circuits*, vol. 17, no. 3, pp. 522–528, 1982.

[9] P.-H. Hsieh, C.-H. Chou, and T. Chiang, "An RF energy harvester with 44.1% PCE at Input Available Power of of 12 dBm," *IEEE Trans. Circuits and Systems I: Regular Papers*, vol. 62, no. 6, 2015.

[10] P. H. Chen and P. M. Y. Fan, "An 83.4% peak efficiency single-inductor multiple-output based adaptive gate biasing DC-DC converter for thermoelectric energy harvesting," *IEEE Trans. Circuits and Systems I: Regular Papers*, vol. 62, no. 2, pp. 405–412, 2015.

[11] D. Masotti, A. Costanzo, P. Francia, M. Filippi, and A. Romani, "A load-modulated rectifier for RF micropower harvesting with start-up strategies," *IEEE Trans. Microw. Theory Tech.*, vol. 62, no. 4, pp. 994–1004, 2014.

[12] F. Serra-Graells and J. L. Huertas, "Sub-1-V CMOS proportional-to-absolute temperature references," *IEEE J. Solid-State Circuits*, vol. 38, no. 1, pp. 84–88, 2003.